HHS Public Access

Author manuscript

J Invest Dermatol. Author manuscript; available in PMC 2016 July 01.

Published in final edited form as:

J Invest Dermatol. 2016 January ; 136(1): 225–235. doi:10.1038/JID.2015.389.

Connexin26 mutations causing palmoplantar keratoderma and deafness interact with connexin43, modifying gap junction and hemichannel properties

Zunaira Shuja[1,2], **Leping Li**[1], **Shashank Gupta**[3], **Gülistan Meşe**[4], and **Thomas W. White**[1]

[1]Department of Physiology and Biophysics, Stony Brook University, Stony Brook, NY USA

[2]Graduate Program in Genetics, Stony Brook University, Stony Brook, NY USA

[3]InSTAR Program, Ward Melville High School, Setauket, NY USA

[4]Department of Molecular Biology and Genetics, Izmir Institute of Technology, Urla, Izmir Turkey

Abstract

Mutations in GJB2 (Cx26) cause either deafness, or deafness associated with skin diseases. That different disorders can be caused by distinct mutations within the same gene suggests that unique channel activities are influenced by each class of mutation. We have examined the functional characteristics of two human mutations, Cx26-H73R and Cx26-S183F, causing palmoplantar keratoderma (PPK) and deafness. Both failed to form gap junction channels or hemichannels when expressed alone. Co-expression of the mutants with wild-type Cx43 showed a trans-dominant inhibition of Cx43 gap junction channels, without reductions in Cx43 protein synthesis. In addition, the presence of mutant Cx26 shifted Cx43 channel gating and kinetics towards a more Cx26-like behavior. Co-immunoprecipitation showed Cx43 being pulled down more efficiently with mutant Cx26, than wild-type, confirming the enhanced formation of heteromeric connexons. Finally, the formation of heteromeric connexons resulted in significantly increased Cx43 hemichannel activity in the presence of Cx26 mutants. These findings suggest a common mechanism whereby Cx26 mutations causing PPK and deafness trans-dominantly influence multiple functions of wild-type Cx43. They also implicate a role for aberrant hemichannel activity in the pathogenesis of PPK, and further highlight an emerging role for Cx43 in genetic skin diseases.

Introduction

Gap junctions form intercellular channels between adjacent cells (Goodenough and Paul, 2003). The oligomerization of six connexins results in half of a gap junction channel referred to as a hemichannel. Connexins allow small metabolites to flow between cells

Corresponding author: Thomas W. White, Department of Physiology and Biophysics, Stony Brook University, T5-147 Basic Science Tower, Stony Brook, NY 11794-8661, Tel: (631) 444-9683, Fax: (631) 444-3432, thomas.white@stonybrook.edu.

Conflict of Interest

The authors state no conflict of interest.

(Bevans *et al*., 1998; Kanno and Loewenstein, 1964; Lawrence *et al*., 1978; Veenstra, 1996), and their disruption results in deleterious phenotypes in tissues like the cochlea and epidermis (Brissette *et al*., 1994; Caputo and Peluchetti, 1977; Zhao *et al*., 2006).

The basal layer of the epidermis contains proliferating keratinocytes, whose differentiation produces an outward migration of cells into the spinous and granular layers (Blanpain and Fuchs, 2006, 2009). Keratinocytes have many intercellular connections, including gap junctions (Kam *et al*., 1986). Connexins are expressed in the epidermis and the most prominent is Cx43, which is found throughout the basal, spinous and granular layers (Butterweck *et al*., 1994; Di *et al*., 2001; Goliger *et al*., 1996; Guo *et al*., 1992; Risek *et al*., 1992; Salomon *et al*., 1994; Wiszniewski *et al*., 2000).

Mutations in *GJB2*, encoding Cx26, result in syndromic skin diseases including palmoplantar keratoderma (PPK) with deafness, Vohwinkel syndrome (VS), and keratitis ichthyosis deafness syndrome (KID) (Bakirtzis *et al*., 2003; de Zwart-Storm *et al*., 2011a; de Zwart-Storm *et al*., 2011b; Richard *et al*., 2004; van Steensel, 2004; Zelante *et al*., 1997). KID syndrome comprises vascularizing keratitis, deafness, hair follicle deficiencies, and erythrokeratoderma. Patients have repeated cutaneous infections that can produce lethal septicemia (Griffith *et al*., 2006; Janecke *et al*.; Jonard *et al*., 2008) and an increased risk of squamous cell carcinoma (Mazereeuw-Hautier *et al*., 2007). In contrast, the skin phenotype of PPK associated with deafness is largely limited to hyperkeratosis of the palms and soles (Richard *et al*., 1998; Rouan *et al*., 2001). VS is similar to PPK, but includes constriction bands on the digits (pseudoainhum) leading to auto-amputation (Maestrini *et al*., 1999). The mechanism whereby Cx26 mutations result in KID syndrome has been studied extensively (Lee and White, 2009); however, a conclusive determination has yet to be reached for mutations associated with PPK.

We examined functional attributes of two Cx26 mutations associated with PPK, Cx26-H73R and Cx26-S183F (de Zwart-Storm *et al*., 2008a; de Zwart-Storm *et al*., 2008b). We observed a lack of gap junction channel or hemichannel formation by these mutations when expressed alone, yet revealed an ability of these mutations to modify the functional activity of, and associate with Cx43. Furthermore, we observed changes in hemichannel activity and voltage gating due to interactions of Cx34 with mutant proteins. These observations suggest that some syndromic deafness mutations in Cx26 exert their pathological effects through dominant gains of function, and suggest that in the case of PPK, result from a unique association of mutant Cx26 with Cx43.

Results

PPK mutations are non-functional and inhibit wild-type connexins

Cx26-H73R and Cx26-S183F were expressed in *Xenopus* oocytes with other epidermal connexins and gap junctional conductance, G_j, was measured. Control oocytes injected with water showed negligible conductance (G_j = 0.12 μS), while cells with wild-type Cx26 channels had an average G_j of 9.3 μS. Cells expressing Cx26-H73R RNA had conductance levels similar to water injected controls. Cx26-H73R did not display a dominant inhibitory effect on wild-type Cx26, as co-injected cells had a G_j of 9.9 μS (Student's t-test $p>0.05$,

compared to Cx26 alone, Figure 1a). Thus, Cx26-H73R failed to form functional gap junction channels when expressed alone.

We then examined interaction with Cx30 and Cx43. Oocyte pairs expressing wild-type Cx30 channels had high conductance (G_j = 20 μS, $p<0.05$). Cell pairs expressing a mixture of Cx26 and Cx30 also produced a mean conductance of 20 μS. Co-expression of wild-type Cx30 and Cx26-H73R resulted in conductance similar to the wild-type controls (Student's t-test, $p>0.05$, Figure 1b), suggesting that Cx26-H73R failed to functionally suppress Cx30 channels. In contrast, Cx26-H73R had a strong inhibitory effect on Cx43. Oocytes expressing Cx43 alone had a mean conductance of 4.6 μS, and cells with both wild-type Cx26 and Cx43 were also well coupled (G_j = 6.8 μS). Co-expression of Cx26-H73R and Cx43 yielded significantly lower conductance than cell pairs expressing Cx43 alone (G_j = 1.1 μS, $p<0.05$ Student's t-test, Figure 1c), demonstrating a trans-dominant inhibition of Cx43 by Cx26-H73R.

Unlike Cx26-H73R, Cx26-S183F inhibited Cx26. Conductance (G_j = 0.03 μS) measured in oocytes injected with Cx26-S183F alone was the same as control cells, demonstrating loss of functionality. When Cx26-S183F and Cx26 were co-injected, a mean conductance of 3.2 μS resulted, significantly less than Cx26 alone (8.6 μS, Student's t-test, $p<0.05$, Figure 1d). Like Cx26-H73R, Cx26-S183F failed to inhibit Cx30 (Figure 1e). Cx26-S183F also displayed trans-dominant inhibition of Cx43. Cx26-S183F significantly inhibited Cx43 when both were present in oocytes (G_j = 0.62 μS, $p<0.05$ Student's t-test, Figure 1f). Cx26-S183F displayed a potent inhibition of both wild-type Cx26 and Cx43. Finally, neither mutant was able to form functional heterotypic channels with either wild-type Cx26 (Supplemental Figure S1) or Cx43 (Supplemental Figure S2). These data suggested that Cx26-H73R and Cx26-S183F may result in PPK through an interaction between the mutant and Cx43.

PPK mutants alter Cx43 voltage gating

Physical interaction between Cx43 and Cx26-H73R or Cx26-S183F could modify voltage gating. To examine this, gating of Cx43 channels in the presence and absence of mutant Cx26 was analyzed by subjecting oocyte pairs to hyperpolarizing and depolarizing transjunctional potentials (V_j) while recording junctional currents (I_j). I_js of Cx26 channels displayed asymmetric gating at higher voltages as described previously (Barrio *et al*., 1991; Bruzzone *et al*., 2003) (Figure 2a), while the I_js of Cx43 channels decreased more symmetrically in a voltage-dependent manner (Bukauskas *et al*., 2001; Valiunas *et al*., 2001; White *et al*., 1994) (Figure 2b). Channels in cell pairs expressing both Cx43 and Cx26-H73R (Figure 2c) or Cx26-S183F (Figure 2d) behaved differently. Despite the inability of the mutants to form functional channels by themselves, or heterotypic channels with Cx43, they shifted the behavior of Cx43 to a more asymmetrical voltage response, reminiscent of Cx26.

Steady-state gating was quantified by plotting V_j against G_j and fitting a Boltzmann equation. Analysis of the fits of Cx26 and Cx43 showed an asymmetric and symmetric response, respectively (Figure 2e and 2f). Channels containing Cx43 and Cx26-H73R (Figure 2g) or Cx26-S183F (Figure 2h) displayed gating that resembled Cx43 alone, with

additional asymmetric decay at higher potentials. The Boltzmann parameters (Table 1) showed that mixed channels had adopted properties of Cx26, while retaining elements of Cx43 gating. Like Cx43, channels containing both Cx43 and mutant Cx26 had a change in minimum conductance [G_{min}] values between negative and positive V_js. The potential for Cx43 at which G_j was halfway to G_{min} [V_o] were similar at positive and negative V_js. In contrast, mixed channels had asymmetrical V_os. The gain of asymmetry suggests interaction between mutant and wild-type proteins.

Gating kinetics of channels containing Cx43 and mutant Cx26 were also modified. Time constants (τ) were determined by plotting current decay and fitting to a mono-exponential function. Representative current decays at +120mV showed Cx43 channels closed slower (Figure 3a) than channels containing both Cx43 and the mutants (Figure 3b and 3c). Mixed channels containing Cx43 and Cx26-H73R closed 73% faster than Cx43, with mean closure times of 0.24 seconds versus 0.90 seconds. Channels containing Cx43 and Cx26-S183F closed 53% faster, with a mean closure time of 0.42 seconds ($p<0.05$, one way ANOVA, Figure 3d). At potentials of −120 mV, mixed channels had slower channel closure times than wild-type Cx43 (Figure 3e). The acquisition of Cx26-like properties was seen in the kinetics of mixed mutant and Cx43 channels when compared to Cx43 alone. The mutants exhibited a lack of gap junction channel activity when expressed alone, in a homotypic or heterotypic configurations, however, when co-expressed with Cx43 in the same cell, were able to alter the current decay and shift the equilibrium properties of the channel towards a Cx26-like behavior.

Reduced conductance is not due to lack of mutant protein expression

Syntheses of wild-type and mutant connexins were examined by Western blotting. Immunoblotting for Cx26 revealed ~26kDa bands in lanes corresponding to oocytes injected with either Cx26 or Cx26-H73R (Figure 4a, arrowhead). A non-specific band was also detected in all lanes by the Cx26 antibody used (asterisk). The Cx43 antibody showed ~43kDa bands in oocytes injected with Cx43 cRNA, whether alone or in combination with Cx26 or Cx26-H73R (Figure 4b). When the Cx43 blot was re-probed for β-actin, it was detected at similar intensity in all samples, confirming equal protein loading (Figure 4c). Band densitometry on replicate blots ($n=4$) revealed no significant differences between the expression of Cx26 alone, Cx26-H73R alone, and the wild-type and mutant in combination with wild-type Cx43 ($p<0.05$, Figure 4d). The plot for the normalized intensity of Cx43 protein also failed to show significant differences between the samples ($p<0.05$, one way ANOVA, Figure 4e).

In contrast, Cx26-S183F showed reduced expression compared to Cx26 (Figure 4f). Immunoblotting for Cx43 revealed equivalent protein levels (Figure 4g), thereby attributing the loss of functional activity in the presence of Cx26-S183F to a mechanism not related to the translational efficiency of Cx43. The blot was re-probed for β-actin to ensure equal loading of samples (Figure 4h). Quantification showed that Cx26-S183F was reduced by ~75% compared to Cx26 ($p<0.05$, one way ANOVA, Figure 4i). The reduction in mutant protein indicated either reduced translational efficiency, or protein stability. Examination of Cx43 band intensity showed equivalent expression in all corresponding lanes (Figure 4j).

Although Cx26-S183F expression was lower than Cx26 or Cx26-H73R, the potency with which the mutant was able to affect Cx43 remained high.

Cx26 PPK mutants associate with Cx43

PPK mutants affected the behavior of Cx43, suggesting the possible formation of heteromeric channels. To investigate this, co-immunoprecipitation was performed on cells co-expressing Cx43 and mutant Cx26. Cell lysates showed Cx26 protein present in all lanes containing wild-type or mutant (Figures 5a and 5e). Re-probing for Cx43 revealed similar expression of protein in lanes containing Cx43 alone, or co-expressed with wild-type or mutant Cx26 (Figures 5b and 5f). Immunoblotting the immunoprecipitate revealed Cx26 protein in samples injected with either wild-type or mutant (Figures 5c and 5g). As described above, Cx26-S183F expression was lower than wild-type Cx26 or Cx26-H73R. Immunoprecipitates were reprobed to determine if the Cx26 mutants interacted with Cx43. As previously described (Gemel *et al*., 2004; Yum *et al*., 2010), Cx26 inefficiently co-immunoprecipitated Cx43. Levels of Cx43 protein in the samples co-expressing Cx43 and either Cx26 mutant were much higher, suggesting the mutant proteins were able to more efficiently co-immunoprecipitate with Cx43 (Figures 5d and 5h). These findings show association of mutant Cx26 and Cx43 in heteromeric connexons, providing a potential mechanism whereby mutant Cx26 was able to modify Cx43 activity.

Cx26 PPK mutants do not form functional hemichannels

KID syndrome mutations routinely form active hemichannels (Gerido *et al*., 2007; Mhaske *et al*., 2013; Sanchez *et al*., 2010; Stong *et al*., 2006), however, it is not known if PPK mutations behave similarly. Thus, hemichannel activity was analyzed by expression of Cx26, Cx26-H73R and Cx26-S183F in single oocytes. Water injected control oocytes showed limited current flow at all voltage steps (Figure 6a). As previously characterized (Gerido *et al*., 2007; Gonzalez *et al*., 2006; Lee *et al*., 2009; Mhaske *et al*., 2013; Ripps *et al*., 2004; Sanchez *et al*., 2010; Sanchez *et al*., 2013), Cx26 hemichannel activity resulted in outward currents upon depolarization (Figure 6b). Cx26-H73R and Cx26-S183F showed greatly reduced membrane current compared to Cx26 injected cells (Figures 6c and 6d). Mean membrane currents were plotted against membrane voltage to quantify differences in activity. Cx26 expressing cells showed large outward currents that increased with greater depolarization (Figure 6e). At +60mV, Cx26 produced currents that were an order of magnitude larger than controls, as well as both Cx26-H73R and Cx26-S183F mutants ($p<0.05$). The mutant injected cells were indistinguishable from water injected negative control cells, suggesting loss of native hemichannel activity. Co-expression of Cx26-H73R and Cx26-S183F with wild-type Cx26 produced a reduction in hemichannel activity (Supplemental Figure S3).

Cx26 PPK mutants enhance Cx43 hemichannels

Cx26 PPK mutants altered the activity of Cx43 gap junctions through an association of Cx43 with mutant Cx26 in heteromeric hemichannels. Thus, we examined if Cx26 mutants associated with PPK could also alter Cx43 hemichannel activity. Oocytes expressing Cx43 exhibited no hemichannel activity (Figure 6f), as previously reported (White *et al*., 1999).

Although Cx43, Cx26-H73R and Cx26-S183F were all unable to form hemichannels alone, heteromeric hemichannels composed of Cx43 with either Cx26-H73R, or Cx26-S183F, showed significantly higher current flow (Figures 6g and 6h). Quantification of the data indicated a marked increase in hemichannel activity in cells co-expressing Cx26-H73R and Cx43 at increasing voltages, demonstrating acquired hemichannel function (Figure 6i). We observed a similar, albeit less consistent, trend in cells co-expressing Cx26-S183F and Cx43. Of 55 oocytes recorded, 33% (n=18) showed a clear difference in hemichannel activity from Cx43 expressing cells, whereas, the remaining cells failed to produce membrane currents greater than controls. Differences between hemichannel currrents produced by Cx43 alone and Cx43 co-expressed with Cx26-H73R, or Cx26-S183F were statistically significant ($p<0.05$, one way ANOVA). Thus, Cx43 and the mutants Cx26-H73R and Cx26-S183F were able to form functional hemichannels when co-expressed as heteromeric connexons.

Discussion

We studied two Cx26 mutations associated with PPK and deafness. Cx26-H73R and Cx26-S183F were unable to form functional homomeric hemichannels or gap junctions when expressed alone. However, upon introduction to cells expressing Cx43, they reduced Cx43 gap junctional activity, altered channel gating and increased hemichannel activity. Co-immunoprecipitation of Cx43 and mutant Cx26 showed the formation of heteromeric connexons. This acquired gain of function distinguishes Cx26 mutations associated with PPK from other Cx26 syndromic disorders such as KID syndrome. The ability of both mutants to modify Cx43 hemichannels and gap junctions brings into focus an emerging role of Cx43 in the causation of epidermal disorders, and highlights common attributes of Cx26 mutations linked to PPK.

We previously analyzed the functional properties to three Cx26 mutants causing PPK and deafness, Cx26-R75W, Cx26-8E42 and Cx26-D66H. All of the mutants lacked intrinsic gap junction channel activity, and inhibited co-expressed wild-type Cx26 (Richard *et al*., 1998; Rouan *et al*., 2001). When co-expressed with Cx43, the mutants all produced a strong inhibition of Cx43 coupling (Rouan *et al*., 2001). This model of trans-dominant inhibition of Cx43 was supported by study of the Cx26-G59A mutation associated with PPK and deafness showing that Cx26-G59A failed to form channels by itself, and also inhibited intercellular dye transfer when co-expressed with Cx43 (Thomas *et al*., 2004). Thus, trans-dominant interactions between Cx26 mutations and Cx43 could reduce overall coupling between epidermal keratinocytes, contributing to skin diseases like PPK.

Accumulating data suggests that syndromic Cx26 mutations causing skin disease acquire new functional activities. To date, all tested PPK mutations were devoid of any intrinsic homomeric channel activity. In contrast, KID mutations form constitutively active homomeric hemichannels, and many can form functional homomeric gap junction channels (Gerido *et al*., 2007; Lee *et al*., 2009; Sanchez *et al*., 2010). Thus, two mechanisms have emerged for skin disease linked Cx26 mutations: i) inhibition of other keratinocyte connexins and ii) formation of aberrant hemichannels. Trans-dominant inhibition would decrease the number of connexin types contributing to intercellular communication in the

epidermis. Active hemichannels would produce extracellular release of metabolites, potentially adversely influencing neighboring cells, or initiating apoptosis. Additional characterization of disease causing mutations will further our understanding of the pathophysiology of skin diseases where connexin activity has been compromised.

Cx43 is expressed across the epidermis (Butterweck *et al*., 1994; Kamibayashi *et al*., 1993), and mutant Cx26 expression is upregulated in patients with PPK and co-localizes with Cx43 (Rouan *et al*., 2001). Mutations in *GJA1*, encoding Cx43, result in oculodentodigital dysplasia (ODDD) (Paznekas *et al*., 2003), erythrokeratodermia variabilis et progressiva (EKVP) (Boyden *et al*., 2015), and keratoderma-hypotrichosis-leukonychia totalis syndrome (KHLS) (Wang *et al*., 2015). These disorders share some clinical features with syndromic Cx26 diseases. ODDD manifests with neuropathies, facial and digit abnormalities and occasionally skin disease (Kogame *et al*., 2014). EKVP results in hyperkeratosis and transient figurate patches of erythema. KHLS encompasses severe hyperkeratosis, congenital alopecia and leukonychia.

There are similarities between clinical features observed in patients with Cx26 and Cx43 mutations. The presence of hyperkeratotic lesions on frictional surfaces (palms and soles) points to possible mechanistic similarities through which PPK arises. Additionally, KHLS shares clinical correlations Bart-Pumphrey syndrome, caused by Cx26 mutations, including hyperkeratosis and leukonychia (Bart and Pumphrey, 1967). Despite phenotypic similarities, functional studies of Cx43 mutations need to be completed to establish definitive mechanistic correlations. Expression of the Cx43-G8V mutation resulting in KHLS resulted in the formation of hemichannels, allowing an influx of Ca^{2+} into cells (Wang *et al*., 2015). Aberrant hemichannel formation was frequently observed in KID syndrome, and in heteromeric connexons containing Cx43 and Cx26 PPK mutants (Figure 6). Another recent study demonstrated increased Cx43 hemichannel activity in the presence of the only non-hemichannel forming KID mutation, Cx26-S17F (Garcia *et al*., 2015). Consistent with our data, Cx26-S17F, was unable to form hemichannels or gap junctions alone, but increased Cx43 hemichannel activity when co-expressed. These findings highlight a growing importance of Cx43 in epidermal disorders, resulting not only from mutations in *GJA1*, but also from the *GJB2* gene.

Materials and Methods

In vitro transcription, oocyte microinjection, and pairing

Cx26, Cx30 and Cx43 were cloned into pCS2+ expression vector for functional studies in *Xenopus* oocytes (DeRosa *et al*., 2009; Turner and Weintraub, 1994). Cx26-H73R and Cx26-S183F constructs were prepared by site directed mutagenesis (Horton *et al*., 1990). DNA constructs were cloned into pBlueScript II (Agilent Technologies, Santa Clara, CA) and sequenced prior to subcloning into pCS2+. Constructs were linearized and transcribed using SP6 mMessage mMachine (Ambion, Austin, TX). Oocytes were collected from *Xenopus laevis* females and cultured in in modified Barth's (MB) medium (Mhaske *et al*., 2013). Oocytes were injected with 10ng of antisense *Xenopus* Cx38 oligonucleotide (Barrio *et al*., 1991; Bruzzone *et al*., 1993), followed by connexin transcripts (5ng/cell) alone or in combination. Water injected oocytes served as a negative control. Cx43 RNA was injected

at a concentration that would yield average electrical conductance of ~5–10 μS. Other cRNA was injected at comparable levels.

Recording of hemichannel currents

Hemichannel currents were recorded 24 hours after cRNA injection using a GeneClamp 500 amplifier controlled by a PC-compatible computer through a Digidata 1440A interface using pClamp 8.0 software (Axon Instruments, Foster City, CA). Electrodes (1.5mm diameter glass, World Precision Instruments, Sarasota, FL) were pulled to a resistance of 1–2 MΩ (Narishige, Tokyo, Japan) and filled with 3M KCl, 10mM EGTA, and 10mM HEPES, pH 7.4. Oocytes were recorded in MB medium without added calcium (Gerido *et al*., 2007). Hemichannel current-voltage (I–V) curves were obtained by clamping cells at −40 mV and subjecting them to 5 second depolarizing voltage steps ranging from −30 to +60 mV in 10 mV increments.

Recording of junctional conductance

Junctional conductance (G_j) was measured by initially clamping both cells in a pair at −40 mV (a transjunctional potential (V_j) of zero). One cell was subjected to alternating pulses of ±20 mV and the current produced by the change in voltage was recorded in the second cell, which was equal in magnitude to the junctional current (I_j). Conductance was calculated by dividing I_j by the voltage difference, $G_j = I_j/(V1\text{-}V2)$ (Spray *et al*., 1981). Gating properties were determined by recording the junctional current in response to hyperpolarizing or depolarizing V_js in 20-mV steps. Steady-state currents (I_{jss}) were measured at the end of the voltage pulse. Steady-state conductance (G_{jss}) was calculated by dividing I_{jss} by V_j, normalized to ±20 mV, and plotted against V_j. Data were fit to a Boltzmann relation: $G_{jss} = (G_{jmax}–G_{jmin})/(1+ \exp [A (V_j–V_0)]) + G_{jmin}$, where G_{jmax} is the maximum conductance, G_{jmin} is the residual conductance, and V_0 is the transjunctional voltage at which $G_{jss} = (G_{jmax}–G_{jmin})/2$. A ($=nq/kT$) represents the number (n) of electron charges (q) moving through the membrane where k is the Boltzmann constant, and T is the absolute temperature.

Western blotting

Oocytes extracts were prepared as previously described (White *et al*., 1992), separated on 12% SDS gels and transferred to nitrocellulose membranes. Blots were blocked with 5% milk 0.1% Tween20 in TBS, probed with polyclonal antibodies against Cx26 or Cx43 (Life Technologies, Carlsbad CA), followed by horseradish peroxidase conjugated secondary antibodies (Jackson Laboratories and GE Healthcare). A monoclonal β-actin antibody (Abcam, Cambridge, MA) was used as a loading control. Band intensities were quantified using ImageJ software. The phosphorylated and non-phosphorylated forms of Cx43 (two bands) were quantified and expressed as a single value.

Co-immunoprecipitation

For cell lysate analysis, the membrane fraction was resuspended in SDS sample buffer. For co-immunoprecipitation, the membrane fraction was resuspended in RIPA buffer (Yum *et al*., 2007). Samples were pre-cleared with protein G agarose beads (Roche, Mannheim, Germany) that had been blocked overnight in 5% BSA-PBS and incubated with a

monoclonal Cx26 antibody (Life Technologies). Protein G agarose beads were added to the samples and incubated. Beads were then washed, boiled in SDS sample buffer and eluted proteins were run on gels. Proteins were detected using polyclonal antibodies against Cx26 or Cx43.

Supplementary Material

Refer to Web version on PubMed Central for supplementary material.

Acknowledgements

This work was supported by the NIH grant R01 AR59505 (TWW) from the NIAMS.

Abbreviations used

Cx	connexin
KID	keratitis-ichthyosis-deafness
PPK	palmoplantar keratoderma

References

Bakirtzis G, Choudhry R, Aasen T, et al. Targeted epidermal expression of mutant Connexin 26(D66H) mimics true Vohwinkel syndrome and provides a model for the pathogenesis of dominant connexin disorders. Hum Mol Genet. 2003; 12:1737–1744. [PubMed: 12837696]

Barrio LC, Suchyna T, Bargiello T, et al. Gap junctions formed by connexins 26 and 32 alone and in combination are differently affected by applied voltage. Proc Natl Acad Sci U S A. 1991; 88:8410–8414. [PubMed: 1717979]

Bart RS, Pumphrey RE. Knuckle pads, leukonychia and deafness. A dominantly inherited syndrome. N Engl J Med. 1967; 276:202–207. [PubMed: 6015974]

Bevans CG, Kordel M, Rhee SK, et al. Isoform composition of connexin channels determines selectivity among second messengers and uncharged molecules. J Biol Chem. 1998; 273:2808–2816. [PubMed: 9446589]

Blanpain C, Fuchs E. Epidermal stem cells of the skin. Annu Rev Cell Dev Biol. 2006; 22:339–373. [PubMed: 16824012]

Blanpain C, Fuchs E. Epidermal homeostasis: a balancing act of stem cells in the skin. Nat Rev Mol Cell Biol. 2009; 10:207–217. [PubMed: 19209183]

Boyden LM, Craiglow BG, Zhou J, et al. Dominant De Novo Mutations in GJA1 Cause Erythrokeratodermia Variabilis et Progressiva, without Features of Oculodentodigital Dysplasia. J Invest Dermatol. 2015; 135:1540–1547. [PubMed: 25398053]

Brissette JL, Kumar NM, Gilula NB, et al. Switch in gap junction protein expression is associated with selective changes in junctional permeability during keratinocyte differentiation. Proc Natl Acad Sci U S A. 1994; 91:6453–6457. [PubMed: 8022804]

Bruzzone R, Haefliger JA, Gimlich RL, et al. Connexin40, a component of gap junctions in vascular endothelium, is restricted in its ability to interact with other connexins. Mol Biol Cell. 1993; 4:7–20. [PubMed: 8382974]

Bruzzone R, Veronesi V, Gomes D, et al. Loss-of-function and residual channel activity of connexin26 mutations associated with non-syndromic deafness. FEBS Lett. 2003; 533:79–88. [PubMed: 12505163]

Bukauskas FF, Bukauskiene A, Bennett MV, et al. Gating properties of gap junction channels assembled from connexin43 and connexin43 fused with green fluorescent protein. Biophys J. 2001; 81:137–152. [PubMed: 11423402]

Butterweck A, Elfgang C, Willecke K, et al. Differential expression of the gap junction proteins connexin45, −43, −40, −31, and −26 in mouse skin. Eur J Cell Biol. 1994; 65:152–163. [PubMed: 7889986]

Caputo R, Peluchetti D. The junctions of normal human epidermis. A freeze-fracture study. J Ultrastruct Res. 1977; 61:44–61. [PubMed: 915975]

de Zwart-Storm EA, Hamm H, Stoevesandt J, et al. A novel missense mutation in GJB2 disturbs gap junction protein transport and causes focal palmoplantar keratoderma with deafness. J Med Genet. 2008a; 45:161–166. [PubMed: 17993581]

de Zwart-Storm EA, Rosa RF, Martin PE, et al. Molecular analysis of connexin26 asparagine14 mutations associated with syndromic skin phenotypes. Exp Dermatol. 2011a; 20:408–412. [PubMed: 21410767]

de Zwart-Storm EA, van Geel M, van Neer PA, et al. A novel missense mutation in the second extracellular domain of GJB2, p.Ser183Phe, causes a syndrome of focal palmoplantar keratoderma with deafness. Am J Pathol. 2008b; 173:1113–1119. [PubMed: 18787097]

de Zwart-Storm EA, van Geel M, Veysey E, et al. A novel missense mutation in GJB2, p.Tyr65His, causes severe Vohwinkel syndrome. Br J Dermatol. 2011b; 164:197–199. [PubMed: 20854437]

DeRosa AM, Mese G, Li L, et al. The cataract causing Cx50-S50P mutant inhibits Cx43 and intercellular communication in the lens epithelium. Exp Cell Res. 2009; 315:1063–1075. [PubMed: 19331825]

Di WL, Rugg EL, Leigh IM, et al. Multiple epidermal connexins are expressed in different keratinocyte subpopulations including connexin 31. J Invest Dermatol. 2001; 117:958–964. [PubMed: 11676838]

Garcia IE, Maripillan J, Jara O, et al. Keratitis-ichthyosis-deafness syndrome-associated cx26 mutants produce nonfunctional gap junctions but hyperactive hemichannels when co-expressed with wild type cx43. J Invest Dermatol. 2015; 135:1338–1347. [PubMed: 25625422]

Gemel J, Valiunas V, Brink PR, et al. Connexin43 and connexin26 form gap junctions, but not heteromeric channels in co-expressing cells. J Cell Sci. 2004; 117:2469–2480. [PubMed: 15128867]

Gerido DA, DeRosa AM, Richard G, et al. Aberrant hemichannel properties of Cx26 mutations causing skin disease and deafness. Am J Physiol Cell Physiol. 2007; 293:C337–C345. [PubMed: 17428836]

Goliger JA, Bruzzone R, White TW, et al. Dominant inhibition of intercellular communication by two chimeric connexins. Clin Exp Pharmacol Physiol. 1996; 23:1062–1067. [PubMed: 8977161]

Gonzalez D, Gomez-Hernandez JM, Barrio LC. Species specificity of mammalian connexin-26 to form open voltage-gated hemichannels. FASEB J. 2006; 20:2329–2338. [PubMed: 17077310]

Goodenough DA, Paul DL. Beyond the gap: functions of unpaired connexon channels. Nat Rev Mol Cell Biol. 2003; 4:285–294. [PubMed: 12671651]

Griffith AJ, Yang Y, Pryor SP, et al. Cochleosaccular dysplasia associated with a connexin 26 mutation in keratitis-ichthyosis-deafness syndrome. Laryngoscope. 2006; 116:1404–1408. [PubMed: 16885744]

Guo H, Acevedo P, Parsa FD, et al. Gap-junctional protein connexin 43 is expressed in dermis and epidermis of human skin: differential modulation by retinoids. J Invest Dermatol. 1992; 99:460–467. [PubMed: 1328400]

Horton RM, Cai ZL, Ho SN, et al. Gene splicing by overlap extension: tailor-made genes using the polymerase chain reaction. Biotechniques. 1990; 8:528–535. [PubMed: 2357375]

Janecke AR, Hennies HC, Gunther B, et al. GJB2 mutations in keratitis-ichthyosis-deafness syndrome including its fatal form. Am J Med Genet A. 2005; 133A:128–131. [PubMed: 15633193]

Jonard L, Feldmann D, Parsy C, et al. A familial case of Keratitis-Ichthyosis-Deafness (KID) syndrome with the GJB2 mutation G45E. Eur J Med Genet. 2008; 51:35–43. [PubMed: 18024254]

Kam E, Melville L, Pitts JD. Patterns of junctional communication in skin. J Invest Dermatol. 1986; 87:748–753. [PubMed: 3537149]

Kamibayashi Y, Oyamada M, Oyamada Y, et al. Expression of gap junction proteins connexin 26 and 43 is modulated during differentiation of keratinocytes in newborn mouse epidermis. J Invest Dermatol. 1993; 101:773–778. [PubMed: 8245504]

Kanno Y, Loewenstein WR. Low-Resistance Coupling between Gland Cells. Some Observations on Intercellular Contact Membranes and Intercellular Space. Nature. 1964; 201:194–195. [PubMed: 14118280]

Kogame T, Dainichi T, Shimomura Y, et al. Palmoplantar keratosis in oculodentodigital dysplasia with a GJA1 point mutation out of the C-terminal region of connexin 43. J Dermatol. 2014; 41:1095–1097. [PubMed: 25388818]

Lawrence TS, Beers WH, Gilula NB. Transmission of hormonal stimulation by cell-to-cell communication. Nature. 1978; 272:501–506. [PubMed: 211417]

Lee JR, Derosa AM, White TW. Connexin mutations causing skin disease and deafness increase hemichannel activity and cell death when expressed in Xenopus oocytes. J Invest Dermatol. 2009; 129:870–878. [PubMed: 18987669]

Lee JR, White TW. Connexin-26 mutations in deafness and skin disease. Expert Rev Mol Med. 2009; 11:e35. [PubMed: 19939300]

Maestrini E, Korge BP, Ocana-Sierra J, et al. A missense mutation in connexin26, D66H, causes mutilating keratoderma with sensorineural deafness (Vohwinkel's syndrome) in three unrelated families. Hum Mol Genet. 1999; 8:1237–1243. [PubMed: 10369869]

Mazereeuw-Hautier J, Bitoun E, Chevrant-Breton J, et al. Keratitis-ichthyosis-deafness syndrome: disease expression and spectrum of connexin 26 (GJB2) mutations in 14 patients. Br J Dermatol. 2007; 156:1015–1019. [PubMed: 17381453]

Mhaske PV, Levit NA, Li L, et al. The human Cx26-D50A and Cx26-A88V mutations causing keratitis-ichthyosis-deafness syndrome display increased hemichannel activity. Am J Physiol Cell Physiol. 2013; 304:C1150–C1158. [PubMed: 23447037]

Paznekas WA, Boyadjiev SA, Shapiro RE, et al. Connexin 43 (GJA1) mutations cause the pleiotropic phenotype of oculodentodigital dysplasia. Am J Hum Genet. 2003; 72:408–418. [PubMed: 12457340]

Richard G, Brown N, Ishida-Yamamoto A, et al. Expanding the phenotypic spectrum of Cx26 disorders: Bart-Pumphrey syndrome is caused by a novel missense mutation in GJB2. J Invest Dermatol. 2004; 123:856–863. [PubMed: 15482471]

Richard G, White TW, Smith LE, et al. Functional defects of Cx26 resulting from a heterozygous missense mutation in a family with dominant deaf-mutism and palmoplantar keratoderma. Hum Genet. 1998; 103:393–399. [PubMed: 9856479]

Ripps H, Qian H, Zakevicius J. Properties of connexin26 hemichannels expressed in Xenopus oocytes. Cell Mol Neurobiol. 2004; 24:647–665. [PubMed: 15485136]

Risek B, Klier FG, Gilula NB. Multiple gap junction genes are utilized during rat skin and hair development. Development. 1992; 116:639–651. [PubMed: 1289057]

Rouan F, White TW, Brown N, et al. trans-dominant inhibition of connexin-43 by mutant connexin-26: implications for dominant connexin disorders affecting epidermal differentiation. J Cell Sci. 2001; 114:2105–2113. [PubMed: 11493646]

Salomon D, Masgrau E, Vischer S, et al. Topography of mammalian connexins in human skin. J Invest Dermatol. 1994; 103:240–247. [PubMed: 7518858]

Sanchez HA, Mese G, Srinivas M, et al. Differentially altered Ca2+ regulation and Ca2+ permeability in Cx26 hemichannels formed by the A40V and G45E mutations that cause keratitis ichthyosis deafness syndrome. J Gen Physiol. 2010; 136:47–62. [PubMed: 20584891]

Sanchez HA, Villone K, Srinivas M, et al. The D50N mutation and syndromic deafness: altered Cx26 hemichannel properties caused by effects on the pore and intersubunit interactions. J Gen Physiol. 2013; 142:3–22. [PubMed: 23797419]

Spray DC, Harris AL, Bennett MV. Equilibrium properties of a voltage-dependent junctional conductance. J Gen Physiol. 1981; 77:77–93. [PubMed: 6259274]

Stong BC, Chang Q, Ahmad S, et al. A novel mechanism for connexin 26 mutation linked deafness: cell death caused by leaky gap junction hemichannels. Laryngoscope. 2006; 116:2205–2210. [PubMed: 17146396]

Thomas T, Telford D, Laird DW. Functional domain mapping and selective trans-dominant effects exhibited by Cx26 disease-causing mutations. J Biol Chem. 2004; 279:19157–19168. [PubMed: 14978038]

Turner DL, Weintraub H. Expression of achaete-scute homolog 3 in Xenopus embryos converts ectodermal cells to a neural fate. Genes Dev. 1994; 8:1434–1447. [PubMed: 7926743]

Valiunas V, Gemel J, Brink PR, et al. Gap junction channels formed by coexpressed connexin40 and connexin43. Am J Physiol Heart Circ Physiol. 2001; 281:H1675–H189. [PubMed: 11557558]

van Steensel MA. Gap junction diseases of the skin. Am J Med Genet C Semin Med Genet. 2004; 131C:12–19. [PubMed: 15468169]

Veenstra RD. Size and selectivity of gap junction channels formed from different connexins. J Bioenerg Biomembr. 1996; 28:327–337. [PubMed: 8844330]

Wang H, Cao X, Lin Z, et al. Exome sequencing reveals mutation in GJA1 as a cause of keratoderma-hypotrichosis-leukonychia totalis syndrome. Hum Mol Genet. 2015; 24:243–250. [PubMed: 25168385]

White TW, Bruzzone R, Goodenough DA, et al. Mouse Cx50, a functional member of the connexin family of gap junction proteins, is the lens fiber protein MP70. Mol Biol Cell. 1992; 3:711–720. [PubMed: 1325220]

White TW, Bruzzone R, Wolfram S, et al. Selective interactions among the multiple connexin proteins expressed in the vertebrate lens: the second extracellular domain is a determinant of compatibility between connexins. J Cell Biol. 1994; 125:879–892. [PubMed: 8188753]

White TW, Deans MR, O'Brien J, et al. Functional characteristics of skate connexin35, a member of the gamma subfamily of connexins expressed in the vertebrate retina. Eur J Neurosci. 1999; 11:1883–1890. [PubMed: 10336656]

Wiszniewski L, Limat A, Saurat JH, et al. Differential expression of connexins during stratification of human keratinocytes. J Invest Dermatol. 2000; 115:278–285. [PubMed: 10951247]

Yum SW, Zhang J, Scherer SS. Dominant connexin26 mutants associated with human hearing loss have trans-dominant effects on connexin30. Neurobiol Dis. 2010; 38:226–236. [PubMed: 20096356]

Yum SW, Zhang J, Valiunas V, et al. Human connexin26 and connexin30 form functional heteromeric and heterotypic channels. Am J Physiol Cell Physiol. 2007; 293:C1032–c1048. [PubMed: 17615163]

Zelante L, Gasparini P, Estivill X, et al. Connexin26 mutations associated with the most common form of non-syndromic neurosensory autosomal recessive deafness (DFNB1) in Mediterraneans. Hum Mol Genet. 1997; 6:1605–169. [PubMed: 9285800]

Zhao HB, Kikuchi T, Ngezahayo A, et al. Gap junctions and cochlear homeostasis. J Membr Biol. 2006; 209:177–186. [PubMed: 16773501]

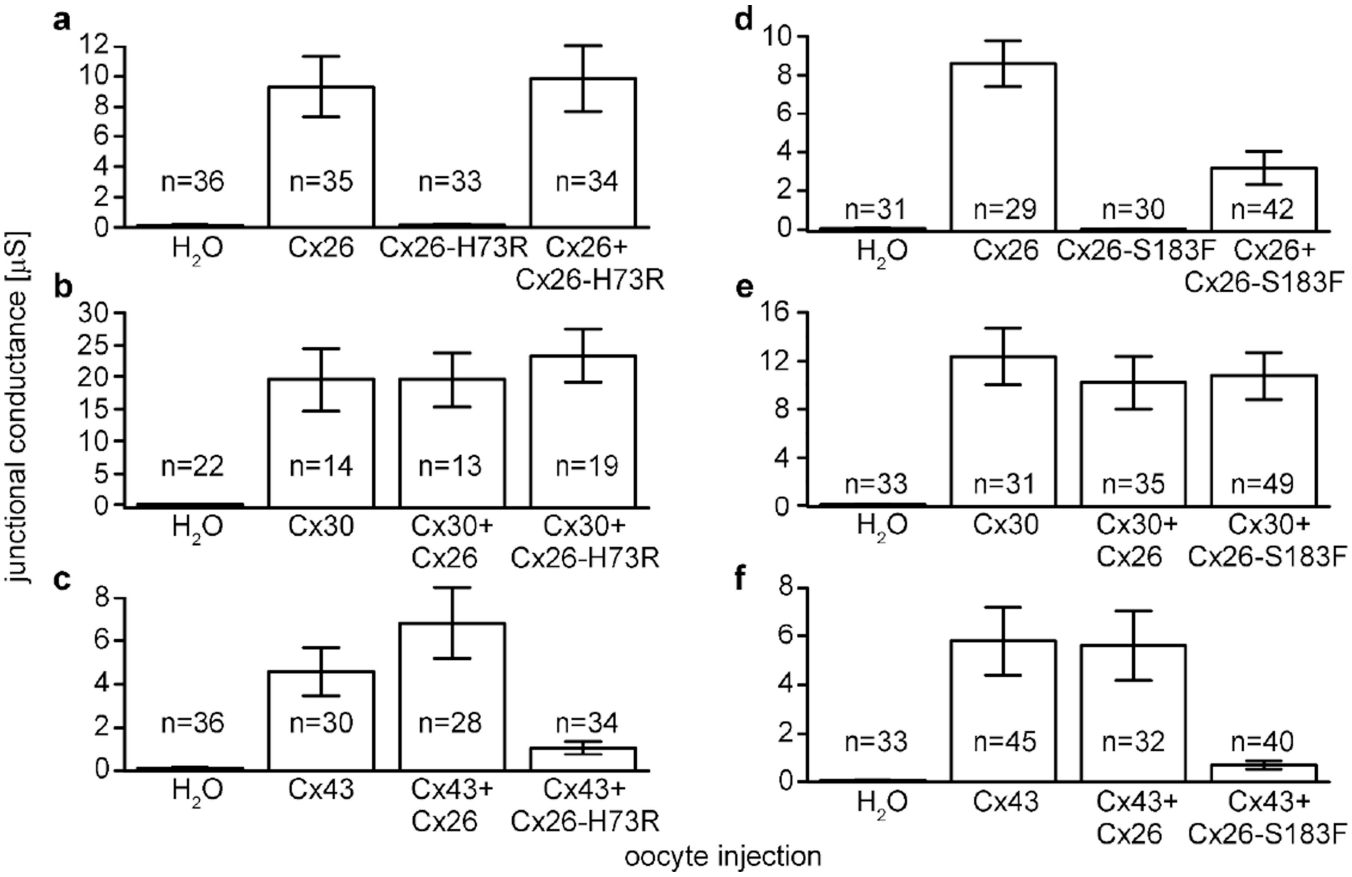

Figure 1. PPK mutations inhibit wild-type Cx43

(a) Water injected cells displayed negligible conductance. Cells expressing Cx26 formed functional channels. Oocytes expressing Cx26-H73R had negligible conductance. Co-expression of Cx26-H73R with Cx26 did not reduce conductance from Cx26 alone. (b) Cx30 formed channels when expressed alone, or in combination with Cx26-H73R. (c) Cx43 formed functional gap junctional channels expressed alone, or with Cx26. The combination of Cx43 and Cx26-H73R produced trans-dominant inhibition of Cx43. (d) Oocytes expressing Cx26-S183F had negligible conductance. Co-expression of Cx26-S183F and Cx26 resulted in a significant decrease in conductance ($p<0.05$) from Cx26 alone. (e) Cx30 formed functional channels when expressed alone or in combination with Cx26-S183F. (f) Co-expression of Cx43 and Cx26-S183F cRNA resulted in a trans-dominant inhibition. Data are the mean ± SE.

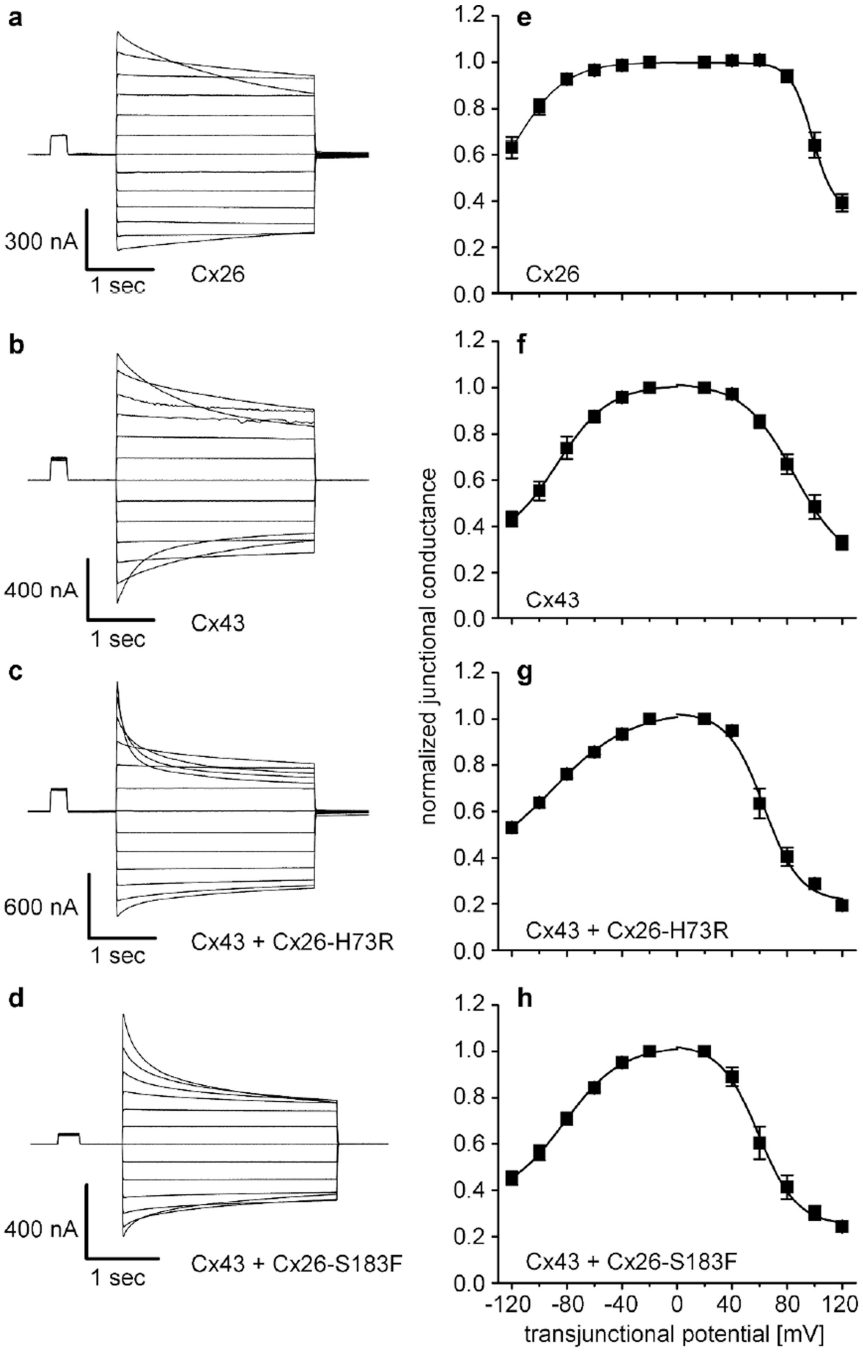

Figure 2. PPK mutants alter voltage gating of Cx43

Recordings of junctional currents in response to transjunctional potentials of opposite polarity revealed that Cx26 (a) showed an asymmetry in current decay at higher voltages, while Cx43 (b) showed a more symmetrical decrease in currents in a voltage-dependent manner. In the presence of Cx26-H73R (c), or Cx26-S183F (d), gating of Cx43 was modified towards a more asymmetrical response to voltage. Quantification of gating by fitting steady state conductance to a Boltzmann equation revealed pronounced asymmetry for Cx26 (e) at negative and positive potentials (n=7). Cx43 (f) showed a more symmetrical

decay (*n*=6). Mixed channels containing Cx26-H73R (g, *n*=4) or Cx26-S183F (h, *n*=7) shifted Cx43 gating properties towards an asymmetrical behavior, reminiscent of Cx26.

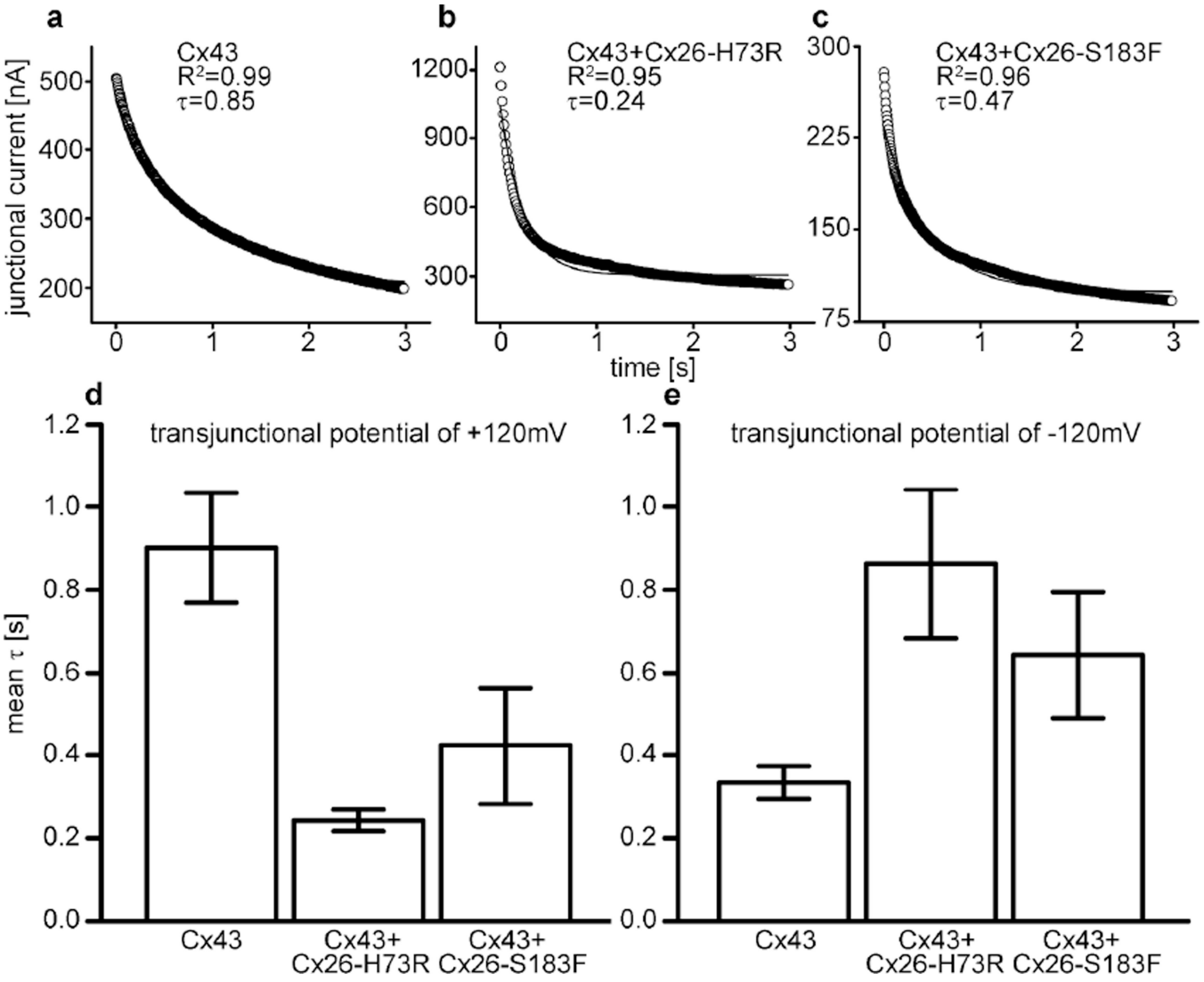

Figure 3. PPK mutants modify Cx43 channel closure kinetics

Junctional currents were fit to a single exponential decay to determine tau (τ). Representative decays at V_j=+120mV showed slower closure kinetics in Cx43 channels (a), while the presence of mutant Cx26-H73R (b), or Cx26-S183F (c), resulted in decreased τ values. (d) At +120mV, mean τ values were 0.90 ± 0.26 for Cx43 alone (*n*=4), 0.24 ± 0.05 for Cx43+Cx26-H73R (*n*=4) and 0.42 ± 0.31 (*n*=5) for Cx43+Cx26-S183F. (e) At −120mV, where Cx43 alone closed faster than it did in the presence of mutant Cx26. Mean τ values were 0.33 ± 0.07 for Cx43 alone (*n*=4), 0.86 ± 0.36 for Cx43+Cx26-H73R (*n*=4) and 0.64 ± 0.34 (*n*=5) for Cx43+Cx26-S183F. Data are the mean ± SE.

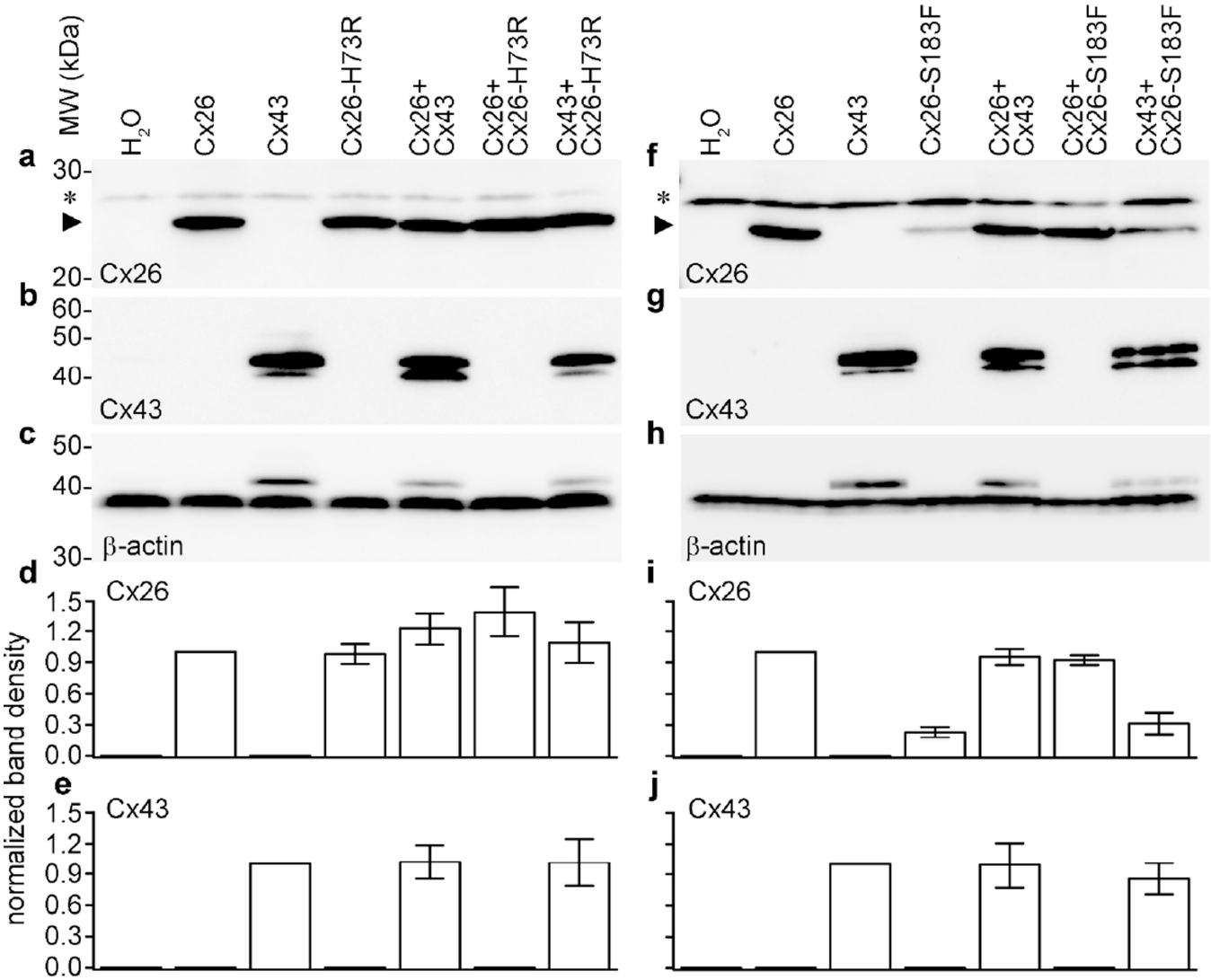

Figure 4. Expression of connexin proteins in Xenopus oocytes

(a) Immunoblot analysis of oocytes expressing Cx26 and Cx26-H73R showed equal expression of protein in all lanes. (b, g) Cx43 levels were the same in each condition. (c, h) Re-probing the Cx43 blots for β-actin confirmed equal loading. (f) Analysis of oocytes expressing Cx26 and Cx26-S183F revealed qualitatively lower expression of the mutant protein as compared to wild-type. (d) Band densitometry (*n*=4) quantitatively confirmed that mean Cx26 and Cx26-H73R protein expression was equivalent in all conditions tested. (e, j) Cx43 levels (n=4) were also equal across experiments. (i) Cx26-S183F protein expression showed a ~75% reduction compared to Cx26 (*n*=4). Data are the mean ± SE.

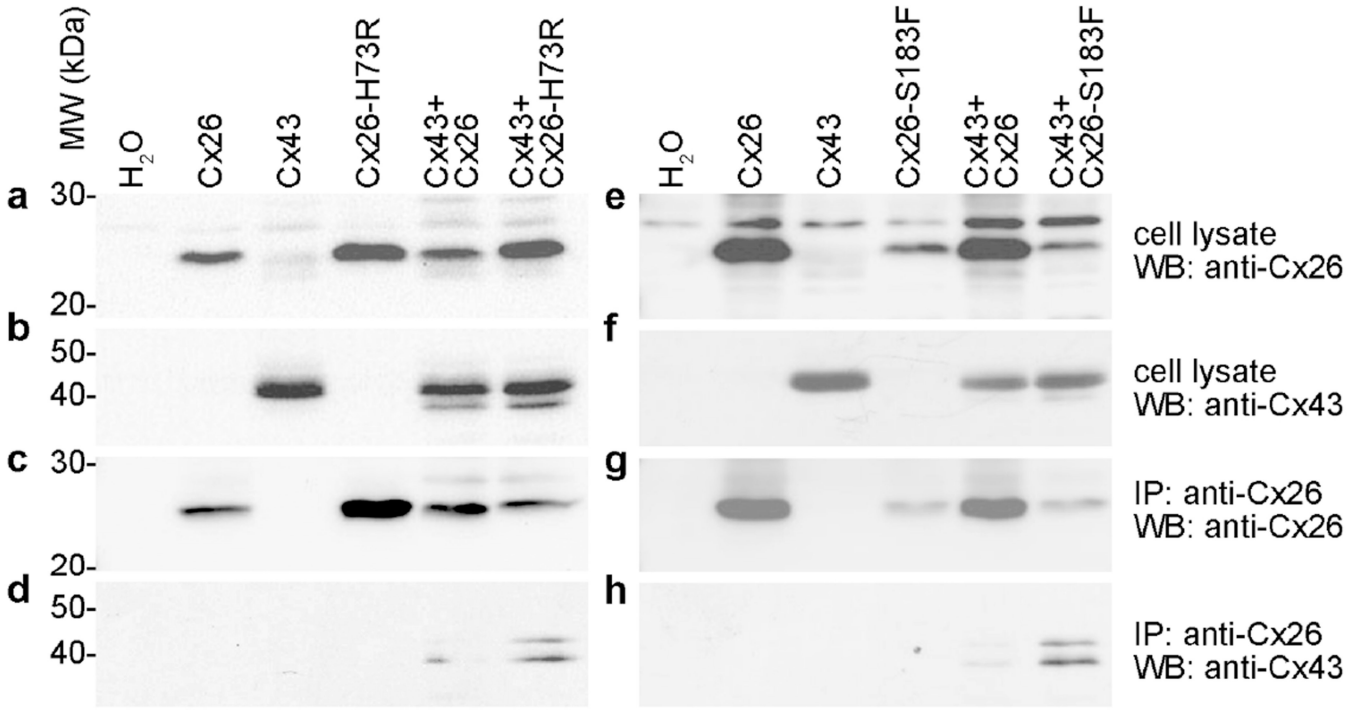

Figure 5. PPK mutants biochemically interact with Cx43

(a, e) Western blot (WB) analysis of cell lysates showed qualitatively similar expression of Cx26 and Cx26-H73R, and reduced protein expression of Cx26-S183F. (b, f) Detection of Cx43 in the cell lysates revealed equal protein expression in corresponding lanes. (c, g) Immunoprecipitation (IP) of Cx26 and subsequent detection of Cx26 protein showed the presence of the protein in all samples containing either wild-type or mutant. (d, h) Co-immunoprecipitation and Western blot analysis of Cx43 revealed enhanced formation of heteromeric channels containing Cx43 and mutant Cx26.

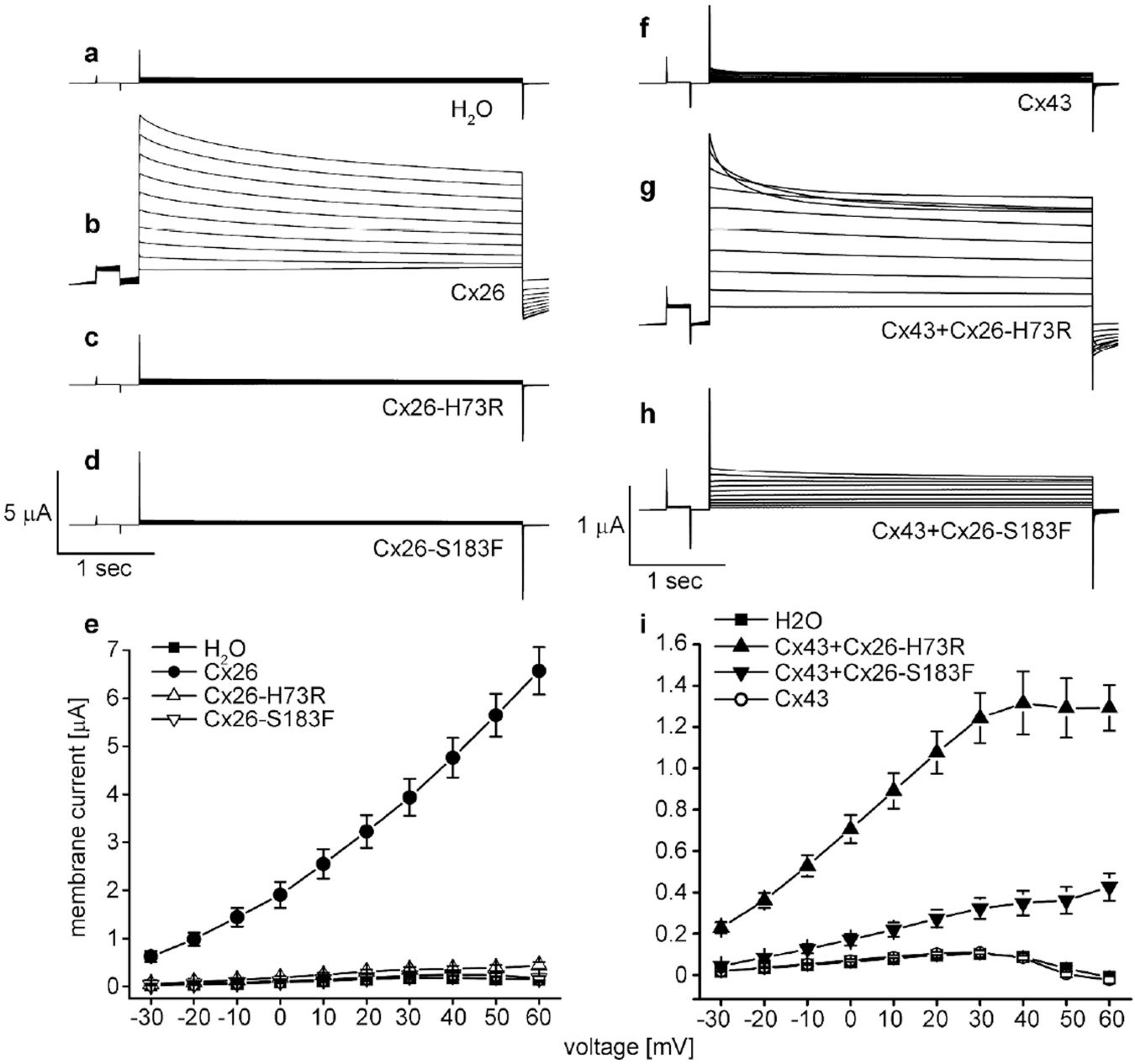

Figure 6. PPK mutants lack hemichannel activity, but stimulate Cx43 hemichannels when co-expressed

(a) Oocytes injected with water exhibited minimal currents. (b) Cx26 cells displayed current that increased at each voltage step. Cx26-H73R (c) and Cx26-S183F (d) lacked hemichannel currents. (e) Steady-state currents for water injected cells were negligible at all voltages (n=12). Cx26 currents increased with depolarization (n=8). Cx26-H73R (n=9) and Cx26-S183F (n=9) currents were negligible. (f) Cx43 cells lacked hemichannel activity. When co-expressed with Cx26-H73R (g), or Cx26-S183F (h), Cx43 showed increased hemichannel activity. (i) Steady-state currents for H_2O (n=21) or Cx43 (n=21) cells were negligible. Co-

expressing Cx43 and Cx26-H73R (n=10) or Cx26-S183F (n=18/55) enhanced Cx43 hemichannel activity. Data are the mean ± SE.

Table 1

Boltzmann parameters of gap junction channels

Oocyte injection	V_j	G_{min}	V_0 [mV]	A
Cx26	+	0.35 ± 0.01	98 ± 0.4	0.13
Cx26	−	0.31 ± 0.14	−118 ± 7.2	0.05
Cx43	+	0.24 ± 0.05	85 ± 2.7	0.05
Cx43	−	0.33 ± 0.03	−87 ± 1.8	0.05
Cx26-H73R+Cx43	+	0.21 ± 0.04	63 ± 3.1	0.08
Cx26-H73R+Cx43	−	0.36 ± 0.09	−90 ± 7.4	0.04
Cx26-S183F+Cx43	+	0.25 ± 0.03	59 ± 2.3	0.07
Cx26-S183F+Cx43	−	0.36 ± 0.04	−82 ± 2.8	0.05

G_{min} represents the minimum conductance value, V_0 indicates the voltage measured midway through the G_j decline, and A denotes the cooperativity constant, reflecting the number of charges moving through the transjunctional field. Signs + and − for V_j indicate transjunctional membrane potential polarity.